Research Article

Small-Size Wide-Band Low-Profile "Pixel Antenna": Comparison of Theoretical and Experimental Results in L Band

Mohamad Rammal [iD],[1] **Mohamad Majed,**[1,2] **Eric Arnaud,**[2] **Joel Andrieu,**[2]
and Bernard Jecko[2]

[1]*ITHPP, Thegra 46500, France*
[2]*XLIM, Limoges 87060, France*

Correspondence should be addressed to Mohamad Rammal; mohamad.rammal@gmail.com

This paper presents a small ($\approx \lambda/2 \times \lambda/2$) low-profile ($\lambda/10$) planar antenna built to work on a very large frequency band ($\geq 40\%$) for applications in Telecom, Radar, IoT, etc. This antenna is called a "Pixel Antenna" because it was first used as a pixel in an agile beam radiating surface. In this paper, the pixel antenna is used alone to design multiband or wide-band antennas keeping the same radiation pattern and polarization throughout the band. The working principle used to design the Pixel Antenna is deduced from the well-known EBG (electromagnetic band gap) antenna in its low-profile version which already has a bandwidth close to $\approx 20\%$. The aim of this present work is to double this bandwidth by simultaneously feeding two modes of the original EBG material. The theoretical and experimental results are compared for an L band application, exhibiting bandwidth from 1 GHz to 1.52 GHz (41%). In addition, good radiation patterns of pixel antenna stay constant over the entire useful band without any degradation of the antenna performance. This proposed antenna design can be used to obtain wide bandwidth for any chosen frequency band (S band, X band, C band, etc.) using frequency scaling.

1. Introduction

In the electromagnetic domain today, applications like telecommunications, radar, IoT, and so on need antennas working on a very large frequency band able to include both Tx and Rx links, to perform frequency hopping, frequency sweeping techniques, pulse generation, and so on.

In the state-of-art wide-bandwidth applications, traveling wave antennas are able to reach 100% bandwidth, but with large dimensions in comparison to the operating wavelength. On the other hand, resonant antennas like patch antennas are usually limited to around 20% bandwidth.

Extensive research has been carried out in the past two to three decades in an attempt to increase the bandwidth of planar antennas. These bandwidth enhancement techniques include use of frequency selective surface (FSS) [1, 2], use of low dielectric substrate, use of multiple resonators, use of thicker substrate [3], employing stacked configuration [4],

and use of slot antenna geometry [5, 6]. Lolit Kumar Singh et al. [7] proposed a T-slot rectangular patch antenna with an impedance bandwidth of 25.23%. Aneesh et al. [8] demonstrated that an S-shaped Microstrip patch antenna can achieve a bandwidth of 21.62%. Mulgi et al. [9] proposed a wideband gap-coupled slot rectangular microstrip array antenna with an impedance bandwidth of 26.72%. Khanna and Srivastava [10] designed a square patch antenna with modified edges and square fractal slots with a bandwidth of 30%.

To further improve the bandwidth of the antenna, i.e., to attain a bandwidth higher than 30%, while respecting the small size, the EBG antenna is the best candidate to increase the bandwidth. A generic EBG antenna consists of a cavity created by a frequency selective surface (FSS) at the top and a metallic ground plane at the bottom. The energy is coupled to the cavity using a feeding antenna such as a dipole, slot, or patch [11, 12]. The EBG antenna has aroused a growing

interest among researchers in the last few years due to its capacity to enhance the directivity of a single source, its potentiality in beam forming, its dual-band frequency, bandwidth enhancement, and its polarization diversity [13–16]. The low-profile pixel antenna, developed from the EBG antenna [17], has a bandwidth limitation of 20%, since it was fed using only one EBG mode.

The novelty of this research work lies in the fact that the dimensions of the pixel antenna are very small compared to those of the EBG antenna and similar to the dimension of the patch antenna: $(\lambda/2) x (\lambda/2)$ with a $\lambda/10$ height (approximately), but the performances in terms of bandwidth are quite different. This is because EBG modes inside the cavity are quasi TEM modes with no variations of such modes in the radial direction.

This paper presents a new technique to increase the frequency band by designing a low profile "Pixel Antenna." The Pixel Antenna is characterized computationally by the commercially available electromagnetic simulation CST Microwave studio software.

2. The "Pixel Antenna" Concept

The high-gain EBG antenna [17], from which the pixel is deduced, is a simple one; a semireflective material (usually FSS) located above a ground plane. The working mode of this structure [17] shows a resonance (f_0) in z direction (Figure 1) like in a Fabry–Perot resonator characterized by:

$$f_0 = \frac{c}{2 \times h_0} \times \left(\frac{\phi_{\sup} + \phi_{\inf}}{2 \times \pi} \right), \tag{1}$$

$$Q = \frac{\sqrt{R_{\sup}}}{1 - R_{\sup}} \times \left(\frac{\phi_{\sup} + \phi_{\inf}}{2} \right), \tag{2}$$

where $R_{\sup}$, $R_{\inf}$, $\phi_{\sup}$, and $R_{\inf}$ are the magnitudes and phases of the reflection coefficients of the upper wall (FSS structure) and of the lower wall (ground plane), respectively. So, normally this height is around $\lambda_0/2$ [17] because the reflection phase of the FSS material usually is near $+\pi$ in the entire frequency band and the reflection phase of the ground plane is equal to π.

For frequencies higher than "f_0," leaky Wave modes and other modes propagate in the structure and the axial directivity evolution as a function of the frequency [17] decreases strongly for $f \geq f_0$.

The frequency band of interest to obtain a directive antenna is characterized by $f \leq f_0$. In this frequency range, the axial directivity of any EBG antenna decreases slowly with the decrease in frequency due to the vanishing behavior of the EM field in the "r" direction inside the structure [17].

If a low-profile EBG antenna [18], characterized by a negative phase of the upper partially reflecting surface [1], is used to design the pixel, the bandwidth highly increases because the quality factor (2) of the resonator strongly decreases [18]. This approach gives a frequency band up to 20% with a suitable feeding technique.

The "pixel antenna" [19] is built from the previous EBG large-size low-profile antenna (Figure 2(a)) by introducing
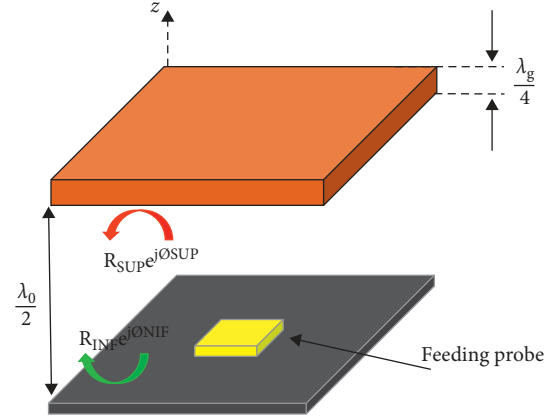

FIGURE 1: Classical EBG antenna fed by a patch.

walls (Figure 2(b)) around the feeding probe (usually a patch) [17]. Figure 3(a) shows the pixel structure with the metallic walls fed by the square patch inside the cavity (Figure 3(b)). Due to the radially vanishing mode, the surface EM field is almost constant on the top of the "pixel antenna" (Figure 3(c)), thus generating a directive radiation pattern [19].

In the following example, the upper semireflective surface is a dielectric slab with FSS pattern. $R_{\sup}$ (f) and $\phi_{\sup}$ (f) are given in the Figure 4.

The lateral dimensions of the pixel are chosen to keep a uniform surface field (Figure 3(c)); they are usually chosen between $0.2\lambda_c$ to $1.2\lambda_c$.

3. Ultra Wide Band Solution

The fundamental objective of this paper is to at least double the previous results ($\approx$20%) by considering a "Pixel Antenna" working on two or more EBG modes.

As mentioned earlier in Section 2, the "pixel antenna" (and also the original EBG antenna [17]) is designed from an EBG material slab built with 2 parallel FSS [17]; a CCE plane has been introduced in the symmetrical plane and the structure is transversally limited by walls.

3.1. Feeding Procedure. The working frequency band for the pixel antenna, deduced from the original EBG antenna, is limited by the "f_0" frequency defined previously in Section 2. Then, for wide bandwidth applications, the central frequency f_c of the expected band is chosen away from this value to have a wide bandwidth not limited by the presence of leaky waves. All the geometrical characteristics of the antenna can be written as a function of the wavelength λ_c corresponding to this frequency (Figure 5) and to obtain a 40% bandwidth, the antenna S_{11} parameter must be less than -10 dB between the two frequencies $0.8\lambda_c$ and $1.2\lambda_c$.

A patch antenna probe used to feed the 2 modes simultaneously is introduced in the structure as shown in Figure 1. The final pixel antenna is shown in Figures 5(a) and 5(b).

An optimization process using CST Microwave Studio software is used to correctly feed the pixel antenna with the
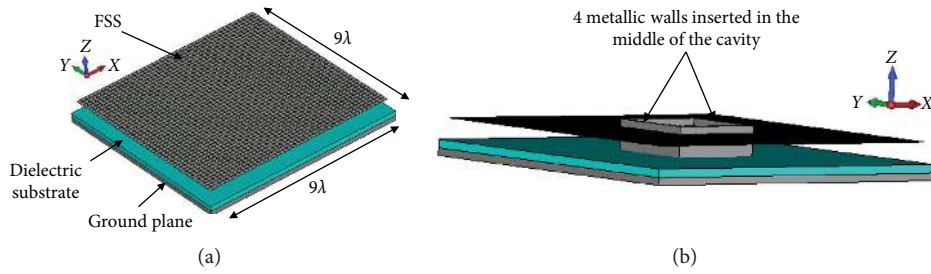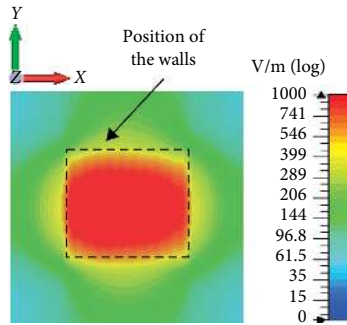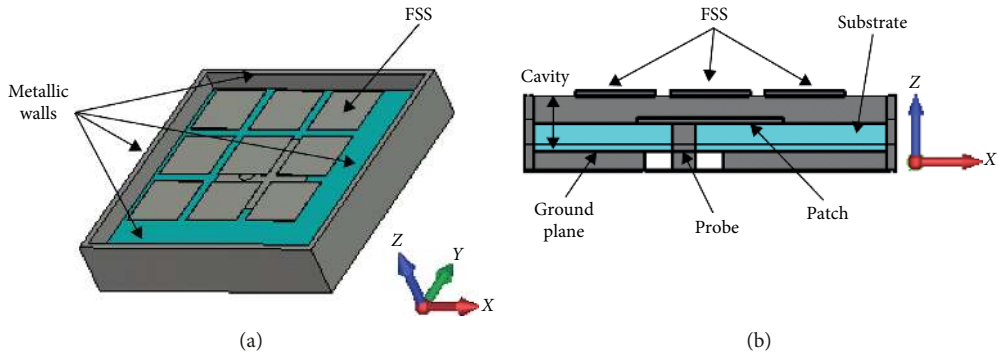
FIGURE 2: (a) High-gain EBG Antenna. (b) Vertical metallic walls inside the EBG antenna.

FIGURE 3: Pixel antenna fed by a patch. (a) Perspective view. (b) Cut view along X-axis. (c) E-field cartography in the top plane.
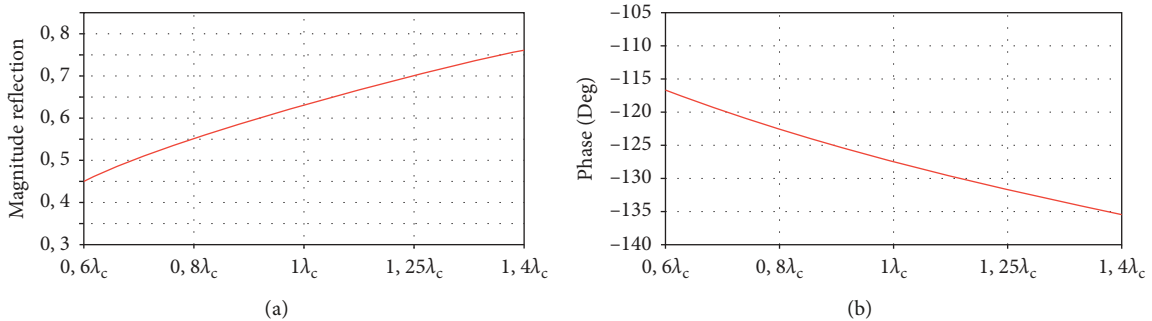

FIGURE 4: Reflection coefficient of a periodic FSS: (a) magnitude; (b) phase.

patch antenna. For example, for such optimizations, consider the S_{11} parameter and impedance evolutions (Figure 6(a)) as a function of the frequency for different patch lengths. When the patch length is varying, the 2 EBG modes are more or less excited. A good compromise is obtained when the length of patch is $0.29\lambda_c$.

It can be observed in another optimization of the resonance frequency versus the height of the cavity, as shown in Figure 6(b), that the second and third resonance frequencies are very sensitive to the variation in the heights of cavity, and it is also seen that we can shift both the second and third resonances towards the first resonance frequency.
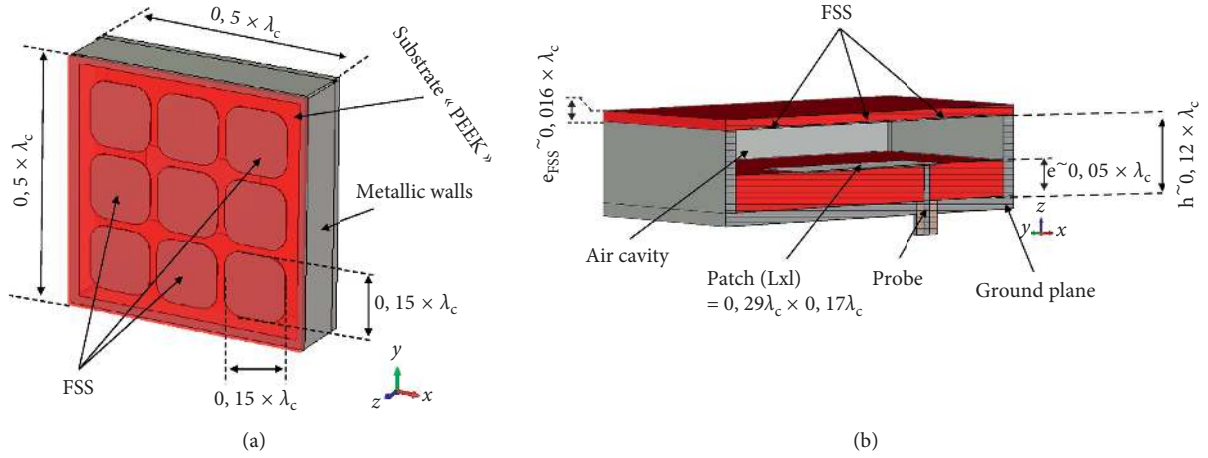
(a)   (b)

FIGURE 5: Pixel antenna design. (a) Perspective view. (b) Cut view along "Y."

(a)   (b)
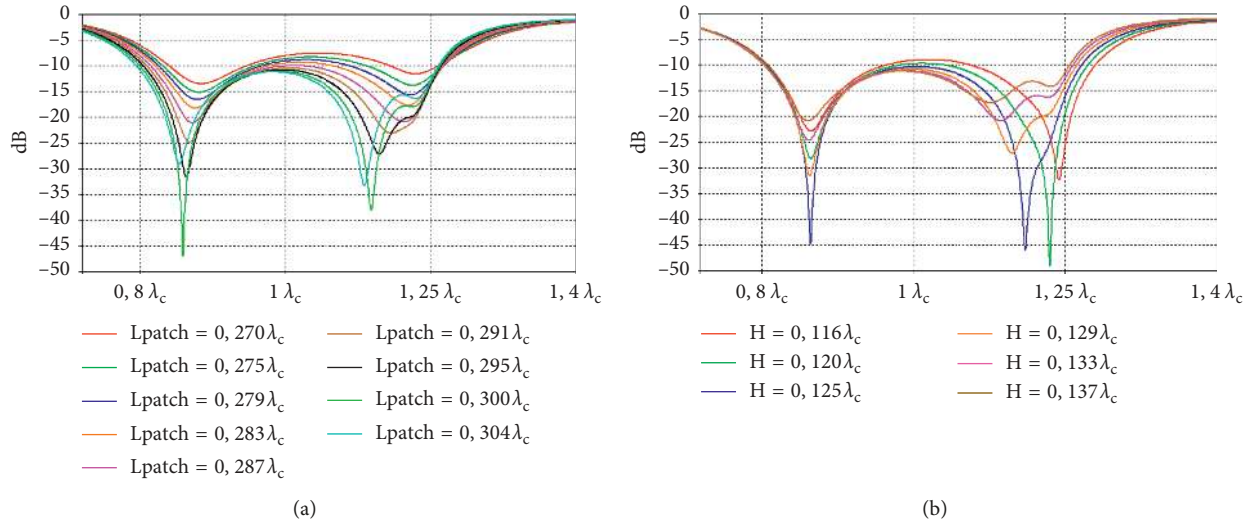
FIGURE 6: (a) S11 parameter evolution vs frequency (theoretical patch resonances when the patch is alone are positioned on the frequency axis when the patch is alone), (b) S11 parameter evolution vs frequency for the height of cavity using patch length (Lpatch) excitation = $0.295\lambda_c$.

It is important to verify that the pixel antenna behaviour remains the same for all the frequencies of the band by showing the electric field cartography on radiating surface (Figure 7) for some frequencies. A uniform radiation surface is obtained on the roof of the pixel antenna generating axial gaussian beams on wide frequency band, approximately 40%.

3.2. Radiation Patterns.
As for EBG antennas [17, 18], the directivity of the antenna and the intrinsic IEEE gain are nearly the same. The difference between the directivity and the IEEE gain is due to the small losses in the dielectric substrate and their frequency evolution (Figure 8) smoothly decreases due to the vanishing effect in the radial direction. This behaviour introduces very wide radiating bandwidth which is limited for high frequencies by the "f_0" given in (1) corresponding to the emergence of the leaky wave.

The antenna is fed by a 50 Ω coaxial cable. As mentioned before, a probe (patch antenna equivalent to a magnetic dipole) is introduced on the ground plane in the middle of the structure (Figure 3), where the impedance of the EM field is near 50 Ω for both the EBG modes.

The realized gain vs frequency band (Figure 8, blue curve) is then limited only by the magnetic dipole emission for low frequencies and by the leaky waves for high frequencies. Consequently, the realized gain exhibits a very large bandwidth (nearly ≈40%).

4. Theoretical and Experimental Results Comparison

To compare the theoretical results with the experimental ones, a frequency band between 1 GHz and 1.5 GHz was chosen.
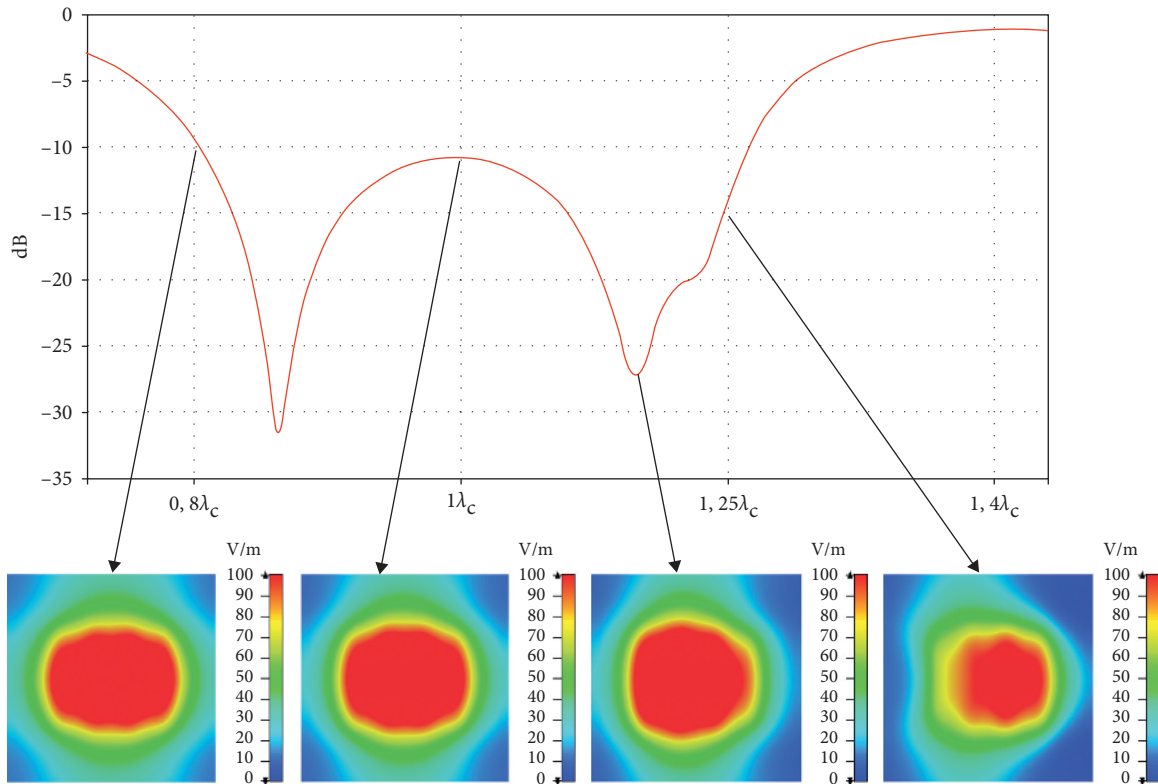
Figure 7: S_{11} parameter vs frequency for a 41% bandwidth and E field cartographies for some frequencies.
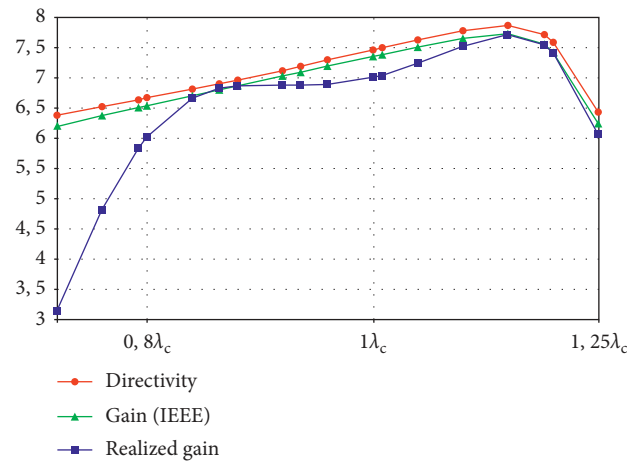

Figure 8: Directivity, intrinsic gain, and realized gain evolutions as a function of frequency.

4.1. Manufactured Structure. Following the geometrical specifications given in Section 3.1, a pixel antenna was designed and manufactured to work between 1 GHz and 1.5 GHz (Figure 9). Because of the wide thickness of the dielectric slab supports, two bulks of PolyEther-Ether-Ketone "PEEK" substrates were used. The metallic patch and the metallic FSS patterns were inserted in these substrates.

4.2. S—Parameters Comparison. The theoretical and experimental S_{11} parameter evolution as a function of the frequency is shown in Figure 10. Both theoretical and experimental results exhibit a wide bandwidth larger than 40%.

4.3. Realized and Experimental Gains Comparison. The theoretical and experimental maximum realized gains vs frequency are compared in Figure 11. The results are in good agreement.

Theoretical and experimental patterns are also very similar for all the frequencies of the band; Figure 12, obtained for the central frequency f_c, illustrates this behaviour.

Figure 13 shows the measured normalized E-plane radiation pattern of the proposed antenna at different
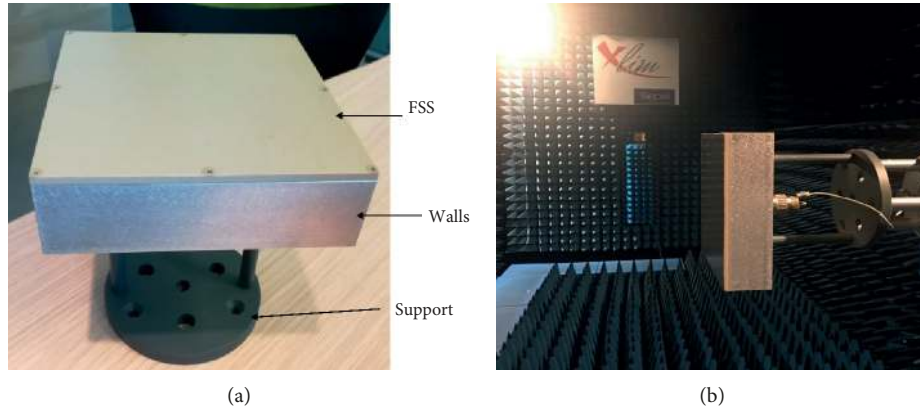
(a)

(b)

FIGURE 9: (a) Pixel antenna with supports. (b) Measurements of the radiation pattern in an anechoic chamber.
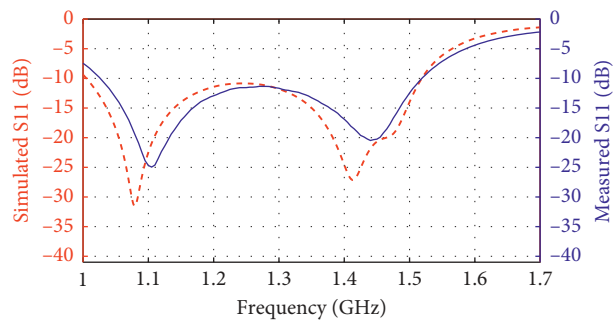

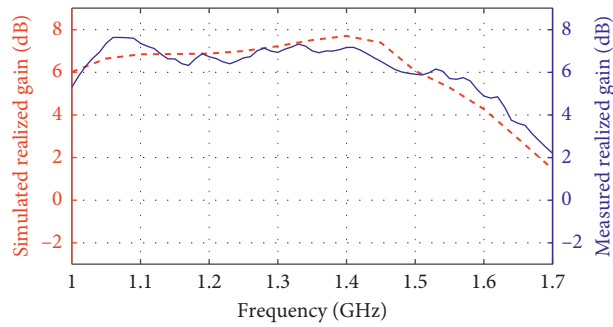FIGURE 10: Theoretical and experimental S_{11} evolution vs frequency.

FIGURE 11: Theoretical and experimental maximum realized gains evolution vs function of the frequency.
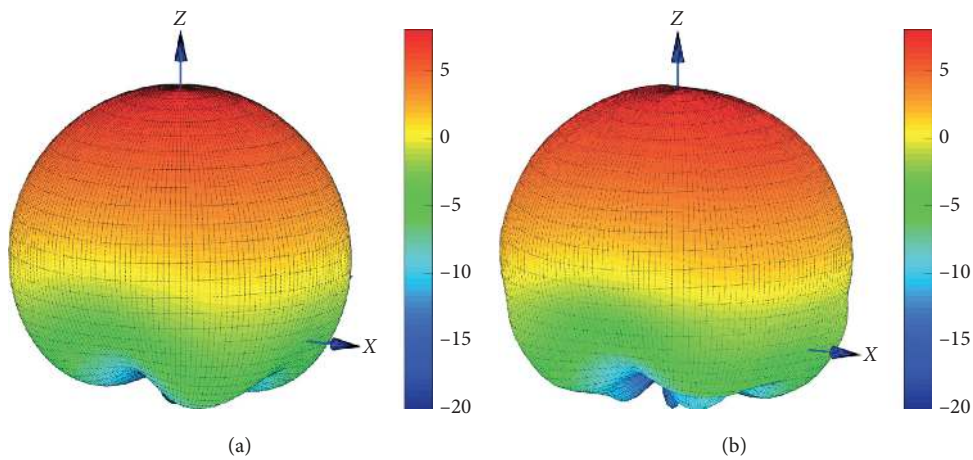

(a)

(b)

FIGURE 12: Theoretical and experimental 3D radiation patterns comparison for a central frequency at 1.25 GHz. (a) Simulation. (b) Measurement.
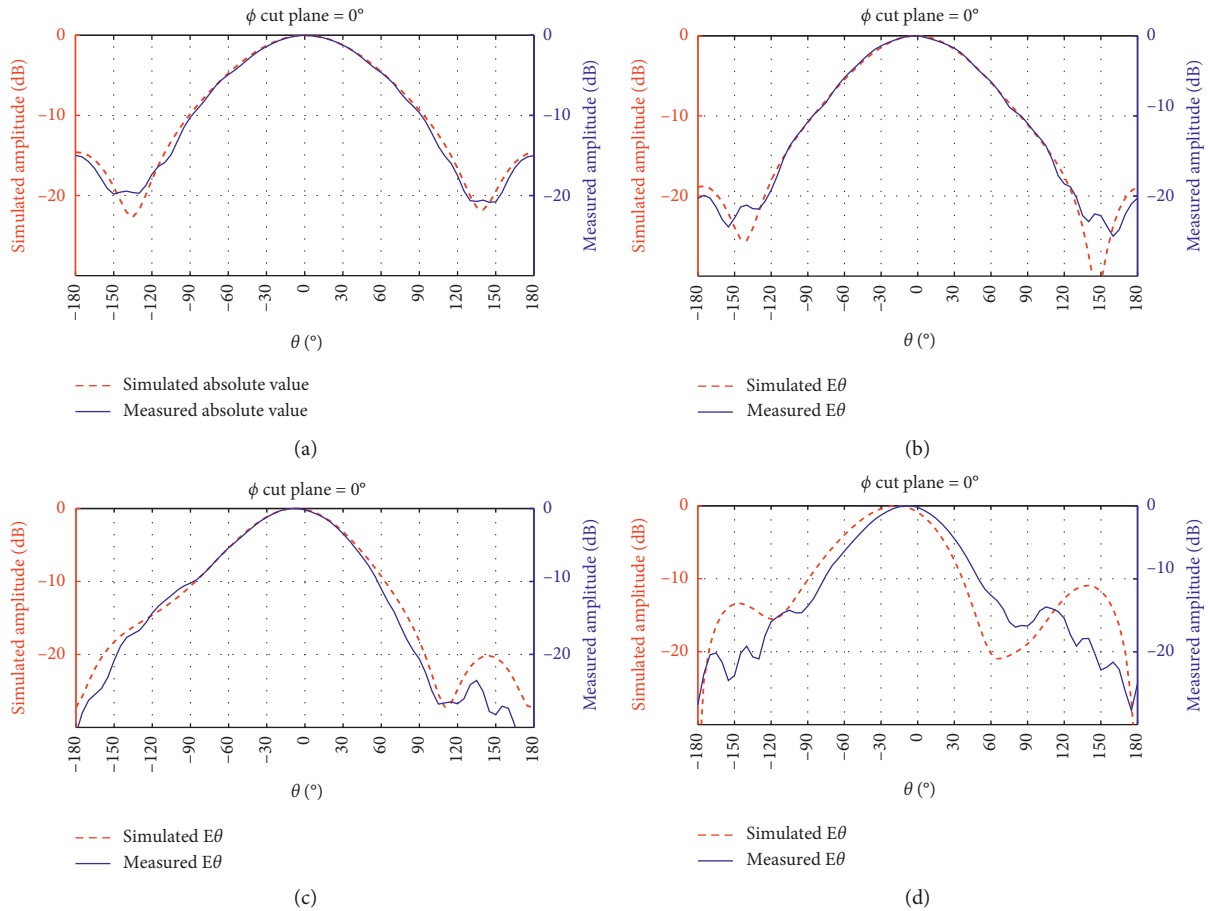
FIGURE 13: Simulation and measurement of the far-field antenna gain (E-plane) at different frequencies: (a) $f = 1$ GHz, (b) $f = 1.25$ GHz, (c) $f = 1.4$ GHz, and (d) $f = 1.5$ GHz.

frequencies. There is good agreement between the simulated and measured radiation patterns at different frequencies.

5. Conclusion

A new kind of antenna called "Pixel Antenna" is introduced in this paper. This antenna is characterized by a very wide frequency bandwidth up to 40%. It has a stable radiation pattern and polarization across the entire band in both linear and circular polarizations [20–22]. Besides the square-shaped surface, the antenna surface can also assume regular shapes like rectangular, circular, trapezoidal, and so on [23].

This antenna can either be used alone or connected to other pixel antennas to build a large radiating surface with a high gain [24], in which case it is called "ARMA" (agile radiating matrix antenna) antennas [19].

Data Availability

Previously reported data were used to support this study, and these prior studies are cited at relevant places within the text as references.

Conflicts of Interest

The authors declare that there are no conflicts of interest regarding publishing this research paper.

References

[1] H.-Y. Chen and Y. Tao, "Performance improvement of a U-slot patch antenna using a dual-band frequency selective surface with modified Jerusalem cross elements," *IEEE Transactions on Antennas and Propagation*, vol. 59, no. 9, pp. 3482–3486, 2011.

[2] H.-Y. Chen and T. Yu, "Antenna gain and bandwidth enhancement using frequency selective surface with double rectangular ring elements," in *Proceedings of the International Symposium on Antenna, Propagation and EM Theory*, pp. 271–274, Guangzhou, China, December 2010.

[3] R. Chair, K. F. Lee, and K. M. Luk, "Bandwidth and cross-polarization characteristics of quarter-wave shorted patch antennas," *Microwave and Optical Technology Letters*, vol. 22, no. 2, pp. 101–103, 1999.

[4] R. B. Waterhouse, "Broadband stacked shorted patch," *Electronics Letters*, vol. 35, no. 2, pp. 98–100, 1999.

[5] K. L. Lau, K. M. Luk, and K. L. Lee, "Design of a circularly-polarized vertical patch antenna," *IEEE Transactions on Antennas and Propagation*, vol. 54, no. 4, pp. 1332–1335, 2006.

[6] D. M. Pozar and D. H. Schauber, *Design of Microstrip Antennas and Arrays*, IEEE Press, New York, NY, USA, 1995.

[7] L. Lolit Kumar Singh, B. Gupta, and P. P. Sarkar, "T-slot rectangular patch antenna," *International Journal of Electronic and Electrical Engineering*, vol. 4, no. 1, pp. 43–47, 2011.

[8] M. Aneesh, J. A. Ansari, A. Singh, and S. S. S. Kamakshi, "Analysis of S-shape microstrip patch antenna for bluetooth applications," *International Journal of Scientific and Research Publications*, vol. 3, no. 11, 2013.

[9] S. N. Mulgi, R. B. Konda, G. M. Pushpanjali, S. K. Satnoor, and P. V. Hunagund, "Design and development of wideband gap-coupled slot rectangular microstrip array antenna," *Indian Journal of Radio & Space Physics*, vol. 37, pp. 291–295, 2008.

[10] A. Khanna and D. K. Srivastava, "Modified edged microstrip square patch antenna with square fractal slots for bluetooth applications," *International Journal of Engineering Research & Technology*, vol. 3, no. 6, pp. 320–323, 2014.

[11] N.G. Alexopoulos and D.R. Jackson, "Fundamental superstrate effects on printed circuit antennas," *IEEE Transactions on Antennas and Propagation*, vol. 32, no. 8, pp. 807–816, 1984.

[12] A. P. Feresidis, G. Goussetis, S. Wang, and J. C. Vardaxoglou, "Artificial magnetic conductor surfaces and their application to low-profile high-gain planar antennas," *IEEE Transactions on Antennas and Propagation*, vol. 53, no. 1, pp. 209–215, 2005.

[13] H. Yang and N. Alexopoulos, "Gain enhancement methods for printed circuit antennas through multiple superstrates," *IEEE Transactions on Antennas and Propagation*, vol. 35, no. 7, pp. 860–863, 1987.

[14] H. Boutayeb and T. A. Denidni, "Metallic cylindrical EBG structures with defects: directivity analysis and design optimization," *IEEE Transactions on Antennas and Propagation*, vol. 55, no. 11, pp. 3356–3361, 2007.

[15] Y. J. Lee, J. Yeo, R. Mittra, and W. S. Park, "Design of a frequency selective surface (FSS) type superstrate for dual-band directivity enhancement of microstrip patch antennas," in *Proceedings of the IEEE Antennas and Propagation Society International Symposium and USNC/URSI Meeting*, pp. 2–5, Washington, DC, USA, July 2005.

[16] H. Yi and S.-W. Qu, "A novel dual-band circularly polarized antenna based on electromagnetic band-gap structure," *IEEE Antennas and Wireless Propagation Letters*, vol. 12, pp. 1149–1152, 2013.

[17] M. Menudier, T. Monediere, and B. Jecko, "EBG resonator antennas: state of art and prospects," in *Proceedings of the 6th International Conference on Antenna Theory and Techniques ICATT'07*, Sevastopol, The Crimea, Ukraine, September 2007.

[18] R. Chantalat, L. Moustafa, M. Thevenot, T. Monédière, and B. Jecko, "Low profile EBG resonator antennas," *International Journal of Antennas and Propagation*, vol. 2009, Article ID 394801, 7 pages, 2009.

[19] B. Jecko, E. Arnaud, H. Abou Taam, and A. Siblini, "The ARMA concept: comparison of AESA and ARMA technologies for agile antenna design," *FERMAT Journal ART*, vol. 20, 2017.

[20] M. S. Toubet, R. Chantalat, M. Hajj, and B. Jecko, "2D matrix of joint ultra low-profile (ULP) EBG antennas for high gain applications," in *Proceedings of the 2012 15th International Symposium on Antenna Technology and Applied Electromagnetics (ANTEM)*, pp. 1–3, Toulouse, France, June 2012.

[21] M. Majed, Y. Sbeity, M. Lalande, and B. Jecko, "Low profile circularly polarized antenna with large coverage for multisensor device links optimisation," in *Proceedings of the Ninth International Conference on Sensor Device Technologies and Applications SENSORDEVICES 2018*, Venice, Italy, September 2018.

[22] A. Siblini, B. Jecko, H. AbouTaam, M. Rammal, and A. Bellion, "New circularly polarized Matrix antenna for space applications," in *Proceedings of the 2016 Wireless Telecommunications Symposium*, London, UK, June 2016.

[23] H. Abou Taam, S. Ali, E. Arnaud, B. Jecko, and M. Rammal, "Matrice antennaire planaire grand gain munie des pixels rayonnants à grandes dimensions $(1.2\lambda \times 1.2\lambda)$," in *Proceedings of the XIXèmes Journées Nationales Microondes*, Bordeaux, France, June 2015.

[24] B. Jecko, M. Majed, S. Aija et al., "Agile beam radiating surfaces," *Source: Fermat*, vol. 30, p. 2, 2018.